

International Union of Pure and Applied Chemistry

11th INTERNATIONAL SYMPOSIUM

ON PLASMA CHEMISTRY

LOUGHBOROUGH UNIVERSITY
LOUGHBOROUGH, LEICESTERSHIRE, ENGLAND.
AUGUST 22 - 27 1993

SYMPOSIUM PROCEEDINGS

VOLUME 4

Edited by J E Harry

NUMERICAL SIMULATION OF DYNAMICS OF LASER PLASMA

V. Mazhukin (*), I. Smurov (**), G. Flamant (***)

(*) Institute of Mathematical Modeling, Academy of Sciences, Moscow, Russia

(**) Ecole Nationale d'Ingénieurs de Saint-Etienne, France

(***) IMP - C.N.R.S., BP 5 Odeillo, 66125 Font-Romeu, Cédex, France

ABSTRACT

The evolution of laser plasma about the threshold values (for plasma formation) of radiation intensity ($q_0 = 5 \cdot 10^7 - 5 \cdot 10^8 \text{ W/cm}^2$; laser wavelength $\lambda = 1.06 \mu\text{m}$) in nitrogen with pressure variation in the range of 3-10 MPa, is analyzed.

I. INTRODUCTION

The dynamics of laser produced plasma and its interaction with laser beam is important to :

- (a) determine the total energy input into irradiated material (that generally depends on: (1) laser radiation passed through plasma cloud; (2) radiative transfer from plasma pattern);
- (b) modify the surface layers of material, for example to create nitrides and carbides coatings [1,2];
- (c) optimize surface evaporation in pulsed laser deposition [3].

The process of laser plasma generation and its subsequent evolution can be divided conditionally into three stages: (a) gas breakdown, (b) opaque plasma exitation, and (c) quasi steady-state distribution of plasma discharges [1-4]. The specific point of the process under consideration is that along with the hydrodynamic mechanism of energy transfer, the mechanism of radiative transport is essential; heat conduction processes are of little consequence. Besides, if the laser pulse is comparatively long (about 0.5 μs), and the radius r_f of the focal spot is comparatively small (about 300 μs), the radial expansion of laser induced plasma need to be taken into account, that leads to 2D problem. It is assumed that the condition of local thermodynamic equilibrium takes place in laser produced plasma.

II. RESULTS AND DISCUSSION.

The mathematical model of the process comprises the system of 2D axisymmetric equations of radiative gas dynamics in Lagrange variables [4]. Laser radiation is incident along the z axis; laser pulse has a rectangular time-profile and Gaussian spatial distribution. It is assumed that the preliminary specified hot region located along the specimen surface is 15 μm thick, and its temperature is 1.8 eV. At the beginning of the pulse, intense absorption of

laser radiation occurs only in the hot region and causes a strong gas dynamic expansion of the material, therewith entailing the exitation of a shock wave in a cold gas.

A. HIGH PRESSURE OF AMBIENT ATMOSPHERE ($P_0=10$ MPa).

Laser radiation (power density $5 \cdot 10^7$ W/cm²) rapidly raises the temperature and pressure in the hot region. By the time $t=5$ ns, the pressure reaches a maximum of $6 \cdot 10^2$ MPa. Later, despite the temperature growth, the pressure in the hot region falls down because the intensive gas dynamic expansion reduces the material density. The shock wave excited in these conditions reaches a maximum velocity $v=1.3$ km/s at time $t=10$ ns (Figure 1). The maximum temperature T_{sw} of the gas of the shock wave reaches 0.36 eV, which is insufficient to initiate intensive absorption of laser radiation. The shock wave is in fact transparent to laser beam, so the conditions are unfavourable for the generation of a laser-supported detonation wave that could effectively shield the target. Since the shock wave velocity v_{sw} is higher than the velocity of the plasma front, v_{pf} , the shock wave breaks away from the hot region. The absorption of radiation occurs near the hot region at about 50 μm from the target. The shock wave decoupled from the energy source begins to decay, its speed and temperature fall rapidly, and by the time $t=0.533$ μs the shock wave dissipates, leaving behind a subsonic perturbation site. Conditionally, the stage of plasma formation terminates at $t=0.533$ μs, when the gas dynamic velocity becomes lower than the sound velocity.

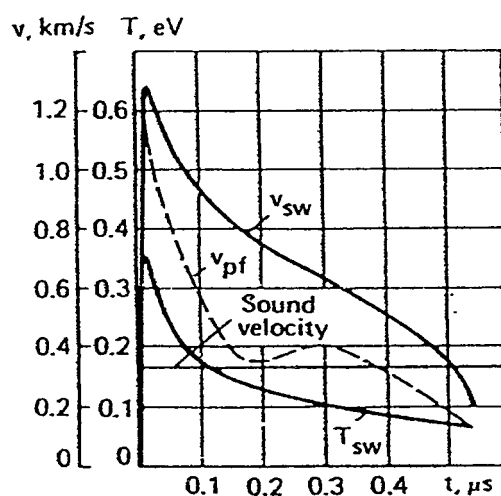


Fig.1. Maximum temperature and speed of a shock wave in gas versus time.

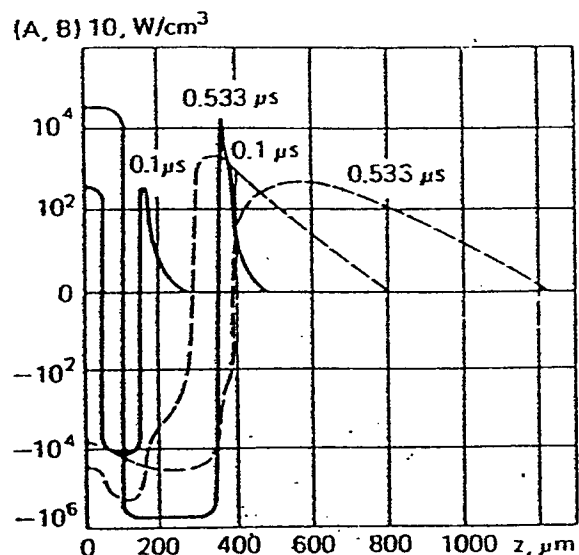


Fig.2. Spatial-temporal distribution of power components in gas due to gas dynamic forces (dashed curves) and radiation transfer (full curves) at $r=0$.

The gas dynamic problem initially is practically one-dimensional, but after a time of about 0.1 μ s the plume extends radially at a rather high speed, and the motion becomes two-dimensional. Since hot layers of nitrogen shield laser radiation from the target, near surface there forms a plasma layer whose temperature is much lower than that of the adjacent upper layer. Two factors are responsible for the shape of the hot region as well as for the shape of the cold region adjacent to the surface : (a) gas dynamic motion; (b) almost complete absorption of laser radiation. The temperature of the region adjacent to the surface gradually falls from 1.8 to 1.1 eV due to shielding of laser radiation and gas dynamic expansion. Starting from $t=15$ ns, plasma products become almost transparent to laser radiation; it is mainly the flux of laser radiation alone (whose incident power density q_e reaches 10^5 W/cm²) that interacts with the target surface. The maximum temperature of the hot region comes to 3.6 eV and does not exceed this limit because the hot region begins to emit radiation much more intensely.

The calculated data show that the area of heat affected zone on the target's surface is a few times larger than the size of focal spot of incident radiation. As follows from the simulation, the process of propagation of plasma products at the initial stage of interaction is transient in character: it progresses from exitation of laser-supported detonation to slow burning. Although the laser-supported detonation process does not influence on, gas dynamic forces contribute markedly to the plasma wave exitation. Figure 2 illustrates the spatial-time distribution of plasma energy components, namely gas-dynamic (A) and radiative (B):

$$A = P \left\{ \frac{1}{r} \frac{\partial}{\partial r} (r u) + \frac{\partial v}{\partial r} \right\}; \quad B = \frac{1}{r} \frac{\partial}{\partial r} (r W_r) + \frac{\partial W_r}{\partial r}$$

Here: r - radial coordinate; u, v - components of velocity vector; P - pressure; W - radiational energy flux.

The amount of energy emitted from the hot region and absorbed by cold nitrogen grows with time, while the amount of energy that goes into gas heating through gas dynamic compression decreases.

B. DECREASE OF PRESSURE OF AMBIENT ATMOSPHERE ($P_0=3$ MPa).

Initially the process of plasma excitation is similar to that observed at 10 MPa. Incident laser radiation, mainly absorbed in the hot zone, leads to an intensive dissipation of the hot plume, followed by the generation of a supersonic wave in time $t=10$ ns, which propagates into the cold gas. The velocity v_{sw}^{max} of the shock wave along the z axis at $r=0$, temperature T_{sw}^{max} , and density ρ_{sw} are 1.9 km/s, 0.36 eV, and $6.1 \cdot 10^{-2}$ g/cm³, respectively.

The profiles of T , p , and ρ of the plasma cloud at $t=0.1$; 0.2; 0.3; and 0.4 μ s, with the shock wave bounded by dash lines, are shown in Figure 3. The

hot plume first extends upward along the z axis. As in the case of laser interaction in nitrogen at 10 MPa, here too the thickness Δz of the hot zone becomes much larger than the absorption length l of a laser light quantum because of the expansion of this zone (Figure 3a). As a result, a major fraction of laser radiation is absorbed in the upper region of the hot zone (region II), while region I adjacent to the target surface is in fact decoupled from laser radiation and at time $t = 0.1 \mu\text{s}$ its temperature T_I is much lower than T_{II} , as seen from Figure 3a. At $t=0.1 \mu\text{s}$, the plume extends radially at appreciable velocities. The effect of gas dynamic expansion of region II at $t=0.1 \mu\text{s}$ is quite apparent. From this time on, the process of plasma formation at 3 and 10 MPa are no longer similar. In view of a lower gas density at 3 MPa, the hot plume in region II dissipates at $t>0.1 \mu\text{s}$ to such an extent that it becomes transparent to laser radiation. The laser pulse now efficiently couples the region I where the nitrogen density ρ_I is higher than ρ_{II} and, hence, the absorptivity is higher too. The rate of expansion of region I grows fast. The profiles of velocities $v(z)$ at $t=0$ are shown in Figure 4, where the region of plume dissipation exhibits a second peak; the first one corresponds to the speed of the shock wave.

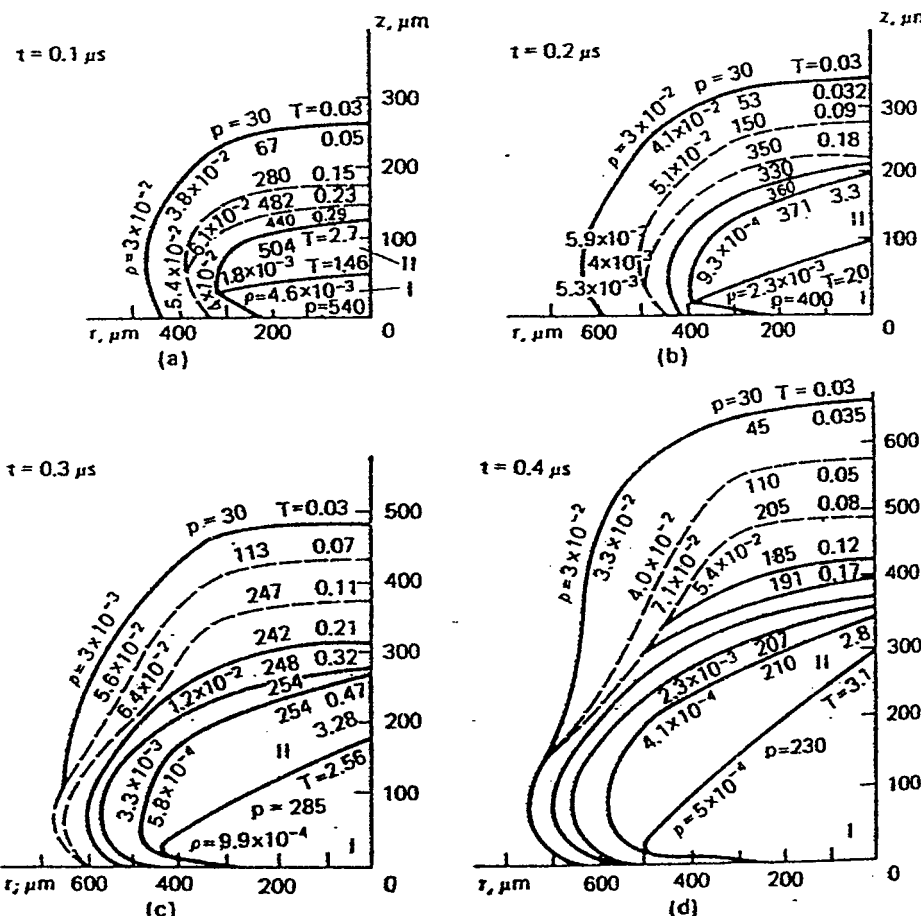


Fig.3. Profiles of temperature, density, and pressure of plasma at $t = 0.1$; 0.2 ; 0.3 ; and $0.4 \mu\text{s}$.

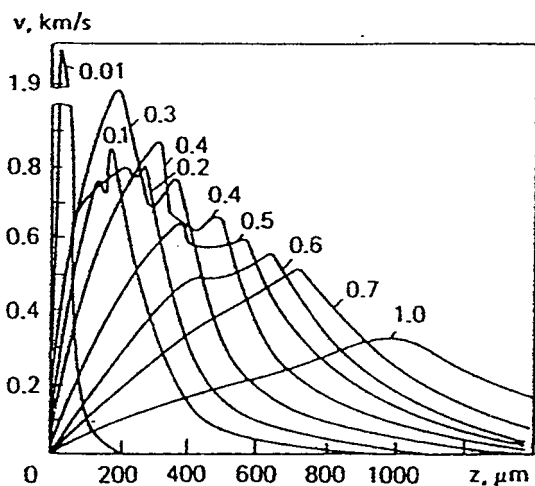


Fig.4. Velocity profiles $v(z)$ at $r=0$ with time (μs) as parameter.

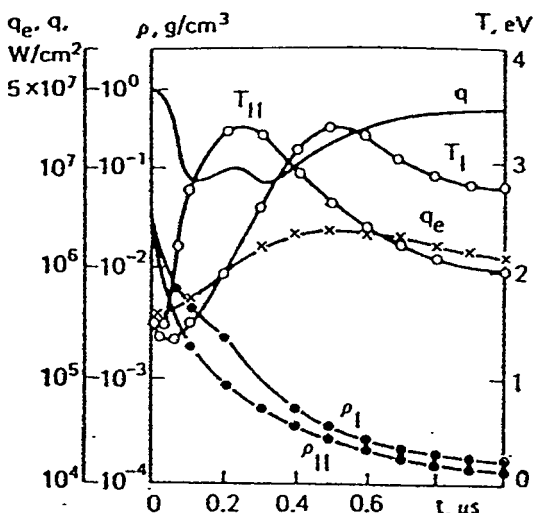


Fig.5. Time dependence of temperatures T_I and T_{II} , plasma densities ρ_I and ρ_{II} , total power density q , and incident irradiance q_e at the target surface.

By the time of the order of $0.3 \mu s$, the spread velocity v of the hot zone approaches a maximum of 1.1 km/s and exceeds the shock wave velocity v_{sw} , which is around 0.75 km/s (Figure 3c). Nevertheless, the second shock under the first does not appear since the plume in region I disperses into region II where the density is lower. The density of the gas within the confines of the shock wave grows from 0.59 g/cm^3 at $t=0.2 \mu s$ to 0.71 g/cm^3 at $t=0.4 \mu s$ (Figure 3d).

The temperature T_{II} (Figure 3) climbs to a maximum of 3.6 eV at $t=0.18 \mu s$ and then drops to 2.0 eV at $t=1 \mu s$ as the plume releases the absorbed energy and attenuates the laser beam to a less extent. The temperature T_I first decreases at $t \approx 0.1 \mu s$ because of the gas dynamic dissipation, but later, as region II gets more transparent and region I absorbs more laser energy, this temperature increases (at $t=0.2; 0.3$ and $0.4 \mu s$) and reaches a maximum of 3.6 eV at $t=0.49 \mu s$. Late in the pulse, as the gas density decreases, the hot zone becomes more transparent, its temperature and pressure fall down, so that the amount of laser energy coupled to the target increases.

The analysis of the contributions of gas dynamic and radiative mechanisms of energy transfer on plasma formation discloses that the first one dominates at the initial stage, $t < 0.2 \mu s$. At $t \approx 0.1 \mu s$, the pulse energy proper that goes into gas heating is merely one tenth that resulting from the work done by the compressive forces. The energy spent on gas dynamic expansion and the plasma-released energy are approximately equal. Even at

$t = 0.3 \mu s$ this ratio changes markedly: 50/1 - becomes the ratio of the energies spent on heating and compression of gas; while the radiation loss becomes 4 times the loss due to expansion. At $t > 0.8 \mu s$, gas dynamic processes are practically negligible. However, the radiant flux delivered to the target decreases with time because of a temperature decrease in region II, as it apparent from Figure 5. The power density of laser beam leaving the region II is $q_e \approx 10^6 \text{ W/cm}^2$, which is almost an order of magnitude higher than that attainable at $p=10 \text{ MPa}$.

It is certainly of importance for laser material processing to know the estimates of laser power density q_e and and the total power density $q(t)$ delivered to the target surface. The q_e coupled to the target surface amounts to $3 \cdot 10^6 \text{ W/cm}^2$ and then drops to $1.6 \cdot 10^6 \text{ W/cm}^2$. The radius of the focal area at $t = 1 \mu s$ is $r_f \approx 600 \mu m$. At $r_f = 250 \mu m$, the curve of q versus time has two clearly defined minima. The first one at $t \approx 0.01 \mu s$ ($q = 6.5 \cdot 10^6 \text{ W/cm}^2$) is indicative of the intensive absorption of laser radiation in region II ($q_p \approx 0.9q$). The second minimum at $t = 0.3 \mu s$ ($q = 6 \cdot 10^6 \text{ W/cm}^2$) results from absorption of laser radiation in region I. Later, as the hot zone becomes transparent due to a decrease in ρ_I and ρ_{II} to 0.14 and 0.13 g/m^3 , respectively, the laser power density delivered to the target surface rises to $3.9 \cdot 10^7 \text{ W/cm}^2$. So, 1 μs after the start of laser pulse, the laser power density delivered to the focal spot reaches about 80% and the plasma cloud does not shield the target surface at an initial nitrogen pressure of 3 MPa.

Calculations show that laser power required to sustain the plasma discharge is practically independent of pressure. The threshold value of power both at 10 and 3b MPa is equal to $q = 4.4 \cdot 10^7 \text{ W/cm}^2$.

III. CONCLUSION.

The utilized approach describes the gas-dynamic stage of laser plasma evolution in a wide range of pressure of ambient atmosphere, and near the threshold values (for plasma formation) of intensity of laser radiation; only some illustrations were presented here. It is possible to determine : different mechanisms of plasma pattern propagation (from laser-supported detonation to slow burning); the total energy flux (including radiative component) reaching the target's surface, etc.

IV. REFERENCES.

1. I. Smurov, A. Smirnov, A. Ferriere, G. Flamant, ISPC-10, Bochum, Germany, 1991, 1.3-7.
2. I. Smurov, A. Uglov, P. Matteazzi, F. Miani, S. Tosto, ISPC-10, Bochum, Germany, 1991, 1.4-28.
3. J. Cheung, J. Horwitz, MRS Bulletin, 17, No. 2, 30 (1992).
4. V. Mazhukin, I. Smurov, G. Flamant, submitted to the J. of Comput. Phys.